

Dipole oscillator strength distributions, sum rules, mean excitation energies, and isotropic van der Waals coefficients for benzene, pyridazine, pyrimidine, pyrazine, *s*-triazine, toluene, hexafluorobenzene, and nitrobenzene

Ajit J. Thakkar^{1, a)}

Department of Chemistry, University of New Brunswick, Fredericton, New Brunswick, Canada E3B 5A3

(Dated: 10 April 2024)

Experimental, theoretical, and additive-model photoabsorption cross-sections combined with constraints provided by the Kuhn-Reiche-Thomas sum rule and the high-energy behavior of the dipole-oscillator-strength density are used to construct dipole oscillator strength distributions for benzene, pyridazine (1,2-diazine), pyrimidine (1,3-diazine), pyrazine (1,4-diazine), *s*-triazine (1,3,5-triazine), toluene (methylbenzene), hexafluorobenzene, and nitrobenzene. The distributions are used to predict dipole sum rules $S(k)$ for $-6 \leq k \leq 2$, mean excitation energies $I(k)$ for $-2 \leq k \leq 2$, and isotropic van der Waals C_6 coefficients. A popular combination rule for estimating C_6 coefficients for unlike interactions from the C_6 coefficients of the like interactions is found to be accurate to better than 1% for 606 of 628 cases (96.4%) in the test set.

I. INTRODUCTION

The current interest in non-covalent interactions has generated renewed efforts to develop improved theoretical methods for the calculation of van der Waals interactions.¹ It is important to have reliable, experiment-based, reference values of the van der Waals dispersion coefficients C_6 to assess these theoretical methods. Since the early insight of Margenau,² the most reliable experiment-based values of C_6 coefficients have been obtained from dipole oscillator strength distributions (DOSDs).

The DOSD of an atom or molecule³ consists of the set of discrete excitation energies E_i and oscillator strengths f_i together with the differential dipole oscillator strength (DOS) function (df/dE) for the continuum of energies $E_c \leq E < \infty$ that begins at the continuum threshold E_c . The DOS is proportional to the photo-absorption cross section, σ . Many constructions of a complete DOSD from experimental data possibly subject to a few constraints have been reported; for a representative sample, see Refs. 4–8.

No complete DOSDs are available for (hetero)aromatic molecules apart from benzene⁹ and pyridine.³ The purpose of this work is to report the construction of constrained DOSDs and the resulting dipole sum rules $S(k)$ for $-6 \leq k \leq 2$, mean excitation energies $I(k)$ for $-2 \leq k \leq 2$, and isotropic van der Waals C_6 coefficients for pyridazine (1,2-diazine, $C_4H_4N_2$), pyrimidine (1,3-diazine, $C_4H_4N_2$), pyrazine (1,4-diazine, $C_4H_4N_2$), *s*-triazine (1,3,5-triazine, $C_3H_3N_3$), toluene (methylbenzene, $C_6H_5CH_3$), hexafluorobenzene (C_6F_6), and nitrobenzene ($C_6H_5NO_2$). Moreover, an improved DOSD is reported for benzene (C_6H_6) because the available DOSD⁹ is now 28 years old and much new experimental photoabsorption data has become available since then.

This work is organized as follows. Section II is a summary of the experimental data, additive models, and methods used to construct the DOSDs. Section III contains a discussion of the resulting DOSDs and molecular properties. Section IV contains some thoughts about the future of DOSD constructions.

II. METHODS AND DATA

A. Experimental data

Photoabsorption measurements for benzene^{10–15} more recent than the 1992 DOSD construction⁹ are available over the extended energy range from 3.76 eV to 200 eV. Experimental photoabsorption data is available for the other molecules only over a smaller energy range, roughly 4 eV to 40 eV. Fortunately, this energy range accounts for 90% or more of the polarizability.^{16,17} Experimental photoabsorption cross-sections are available from 4.4 eV to 40 eV for pyridazine (1,2-diazine),¹⁸ from 3.6 eV to 40 eV for pyrimidine (1,3-diazine),^{19–21} from 4.5 eV to 40 eV for pyrazine (1,4-diazine),^{19,21} from 3.9 eV to 39 eV for *s*-triazine (1,3,5-triazine),^{19,22} from 3.9 eV to 35.6 eV for toluene,^{23–30} and from 4.2 eV to 41.3 eV for hexafluorobenzene.^{31–33} For nitrobenzene, experimental photoabsorption data is available^{26,34–36} for most of the energy range from 3.3 eV to 35.6 eV but there is a gap from 8.1 eV to 9.9 eV. This gap was filled by forward extrapolation of Nagakura *et al.*'s data³⁴ and backward extrapolation of Cooper *et al.*'s data³⁶ to their intersection point at roughly 8.4 eV. Digital files of most of the data mentioned in this paragraph were obtained either from the MPI-Mainz UV/VIS Spectral Atlas³⁷ or the Brion laboratory's database.³⁸

Gas-phase measurements of the molar refractivity can be used as constraints for the constructed DOSDs. However, they are available for only one of the eight molecules considered in this work: benzene.^{39,40}

^{a)} Electronic mail: ajit@unb.ca; <http://people.unb.ca/Ajit.Thakkar/>

B. Additive models

Photoabsorption data is unavailable at higher energies: $E > 200$ eV for benzene, $E > 35$ eV for toluene and nitrobenzene, and $E > 40$ eV for the five other molecules. Additive models are used to approximate this higher energy data.

The simplest additive models are based on free atoms.⁴¹ For all the molecules, photoabsorption cross-sections, σ , were constructed from each of two free-atom additive models. One model, hereafter referred to as A(H), is based on free-atom cross-sections taken from the semiempirical compilation of Henke *et al.*⁴² that extends to 30,000 eV. The other model, hereafter referred to as A(C), is based on the theoretical free-atom cross-sections tabulated by Chantler⁴³ for energies up to 100,000 eV. Atom-additive models are expected to be sufficiently accurate⁴² for $E > 70$ eV but have been used, in favorable circumstances, for energies as low as 15 eV.¹⁶

More elaborate and presumably more accurate additive models⁴¹ can be constructed from molecular fragments (groups) provided that consistent data obtained by the same experimental technique and preferably from the same laboratory is available. Photoabsorption cross-sections, in the region from 25 eV to 200 eV, were generated from two fragment-additive models for all the molecules except benzene. The accuracy of a fragment-additive model depends partly on the choice of the fragments. Chemical intuition can be used to help choose the fragments. For example, the conceptual partition of the target species into fragments should minimize disruption of rings and functional groups.

Since all the molecules studied in this work are closely related to benzene, it makes sense to use benzene as one of the fragments and construct an appropriate correction term from other fragments. Thus we express the cross-section $\sigma(M)$ for molecule M as

$$\sigma(M) = \sigma(\text{benzene}) + \Delta(M) \quad (1)$$

The azines are the most straightforward; bond additivity works reasonably well for their polarizabilities.⁴⁴ Azines differ from benzene by $m = 1, 2, \dots$ aza-substitutions, that is substitutions of C–H by N. Fortunately, experimental cross-sections in the desired energy range are available for both benzene and pyridine, the simplest azine ($m = 1$). The most chemically appealing fragment-additive model used for the m -azines is:

$$\Delta(m\text{-azine}) = m[\sigma(\text{pyridine}) - \sigma(\text{benzene})] \quad (2)$$

which is exact for benzene ($m = 0$) and pyridine ($m = 1$) and should be reasonably accurate for the diazines ($m = 2$) and triazines ($m = 3$). Another fragment-additive model considered for the azines is given by

$$\Delta(m\text{-azine}) = \frac{m}{2}[\sigma(\text{N}_2) - \sigma(\text{C}_2\text{H}_2)]. \quad (3)$$

The available data limits the accessible fragment models for the other three molecules. One fragment-additive

model for hexafluorobenzene is

$$\Delta(\text{C}_6\text{F}_6) = 6[\sigma(\text{CH}_3\text{F}) - \sigma(\text{CH}_4)] \quad (4)$$

and another one is

$$\Delta(\text{C}_6\text{F}_6) = \frac{3}{2}[\sigma(\text{CF}_4) - \sigma(\text{CH}_4)]. \quad (5)$$

For toluene, the two fragment models considered are

$$\Delta(\text{toluene}) = \sigma(\text{propanone}) - \sigma(\text{ethanal}) \quad (6)$$

and

$$\Delta(\text{toluene}) = \sigma(\text{C}_2\text{H}_6) - \sigma(\text{CH}_4). \quad (7)$$

One fragment model used for nitrobenzene is

$$\Delta(\text{nitrobenzene}) = \frac{1}{2}\sigma(\text{C}_2\text{H}_6) - \sigma(\text{CH}_4) + \sigma(\text{NO}_2). \quad (8)$$

A fragment model based on a correction to pyridine rather than benzene is also used for nitrobenzene:

$$\sigma(\text{nitrobenzene}) = \sigma(\text{pyridine}) + \sigma(\text{CO}_2). \quad (9)$$

For the sake of brevity, the fragment-additive model of Eq. (m) is referred to as F(m).

In this work, all the photoabsorption data used for fragment-additive models was taken exclusively from the Brion database³⁸ which contains data for 64 species. The data relevant to this work are unpublished data for propanone and ethanal, and published data for benzene,¹² pyridine,⁴⁵ nitrogen,⁴⁶ ethyne,⁴⁷ methyl fluoride,⁴⁸ nitrogen dioxide,⁴⁹ tetrafluoromethane,⁵⁰ and methane and ethane.⁵¹

C. DOSD construction

A robust method for constructing a DOSD from photoabsorption cross-sections combined with constraints provided by the Kuhn-Reiche-Thomas (KRT) sum rule and usually molar refractivity data was developed,⁵ refined, and applied to more than 50 species by Meath and coworkers as traced in Ref. 52. More recently, the method was augmented by a high-energy constraint based on the asymptotic behavior of the DOS. At first, this technique was restricted to homonuclear molecules^{53,54} but it was later generalized to apply to all molecules.³ Since the initial application of the general method to pyridine,³ it has been applied to 20 more molecules.^{17,55,56}

A terse summary of this method suffices because a detailed description is available elsewhere.³ The available photoabsorption data is divided into energy intervals $[E_i, E_{i+1}]$ for $i = 1, \dots, N$ in which E_1 is the absorption threshold, E_N is the highest energy for which a value of the DOS is available, and $E_{N+1} = \infty$. Then a representative selection is made from the initial distributions that can be constructed using different combinations of

experimental photoabsorption data from diverse sources, additive models, constraints, and a three-term Laurent expansion for the asymptotic region $E > E_N$. The KRT sum rule and the high-energy asymptotic behavior are always used as constraints. Initial values of three parameters that appear in the high-energy constraint³ are obtained from Hartree-Fock values of the electron density at the nucleus, $\rho(0)$, for each of the atoms in the molecule.⁵⁷ Gas-phase molar refractivity values were used as low-energy constraints in some of the distributions for benzene. For each selected distribution, iterations of a constrained least-squares procedure are required to determine simultaneously two parameters in the high-energy constraint³ and the scale factors $1 + a_i$, $i = 1, \dots, N$ for all the energy intervals. Finally, the best DOSD has to be selected. Uniformity of the scale factors is a reflection of the consistency of the initial data and so the distributions that lead to the smallest standard deviations s of the scaling parameters are considered the best. Almost invariably, several DOSDs lead to values of s very close to the lowest value, and then the distribution leading to the smoothest DOS is selected from among these.

D. Property calculations

Once a final DOSD has been selected, quadrature is used to compute the dipole sums $S(k)$ from

$$S(k) = \int_{E_c}^{\infty} dE \left(\frac{df}{dE} \right) E^k, \quad (10)$$

the logarithmic sums $L(k)$ from

$$L(k) = \int_{E_c}^{\infty} dE \left(\frac{df}{dE} \right) E^k \ln E, \quad (11)$$

and the mean excitation energies from:

$$I(k) = \exp(d \ln S(k)/dk) = \exp(L(k)/S(k)). \quad (12)$$

Atomic units are used in the above and following equations. The expression used for the isotropic dipole polarizability $\alpha(\omega)$ at selected frequencies ω is:

$$\alpha(\omega) = \int_{E_c}^{\infty} dE \frac{(df/dE)}{E^2 - \omega^2}. \quad (13)$$

Pseudospectral representations,⁵⁸ $\{\epsilon_i, f_i, i = 1, \dots, 10\}$, of the DOSD are generated from the moments $S(k)$, $-17 \leq k \leq +2$. The pseudospectra are used to compute the C_6 coefficient for long-range interactions between molecules A and B from the venerable expression⁵⁹

$$C_6(A-B) = \frac{3}{\pi} \int_0^{\infty} \alpha_A(iy) \alpha_B(iy) dy \quad (14)$$

in which $i = \sqrt{-1}$.

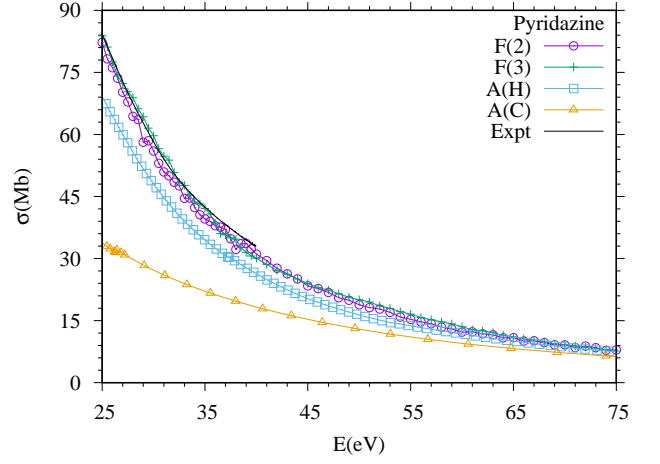


FIG. 1. Photoabsorption cross-sections of pyridazine. The experimental data is from Ref. 18.

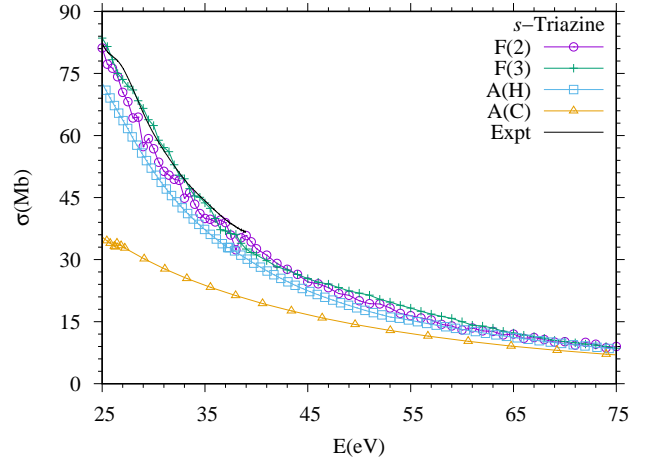


FIG. 2. Photoabsorption cross-sections of *s*-triazine. The experimental data is from Ref. 22.

III. RESULTS AND DISCUSSION

A. How good are the additive models?

Two atom-additive models A(H) and A(C), two applicable fragment-additive models, and experimentally measured cross-sections are compared with one another for pyridazine,¹⁸ *s*-triazine,²² hexafluorobenzene,³³ toluene,²⁷ and nitrobenzene³⁶ in Figs. 1, 2, 3, 4, and 5, respectively.

The figures lead to five general observations.

1. The fragment-additive models $F(m)$ are seen to be reasonably accurate at the lower energies where direct measurements are available. Hence the fragment models $F(m)$ are very likely to be adequate for the somewhat higher energy range $35 \text{ eV} \leq E \leq 200 \text{ eV}$ in which they are used in this work.

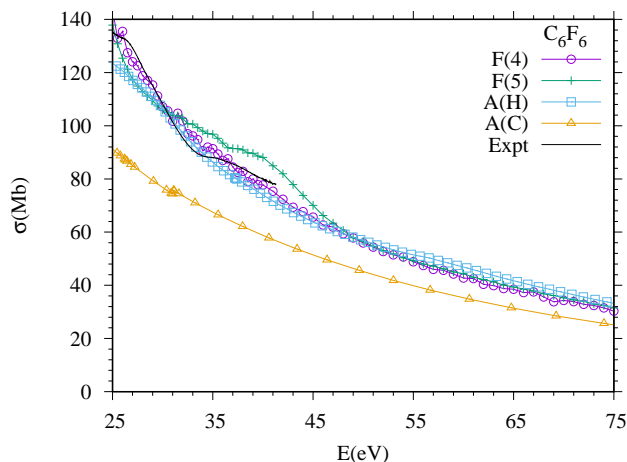


FIG. 3. Photoabsorption cross-sections of hexafluorobenzene. The experimental data is from Ref. 33.

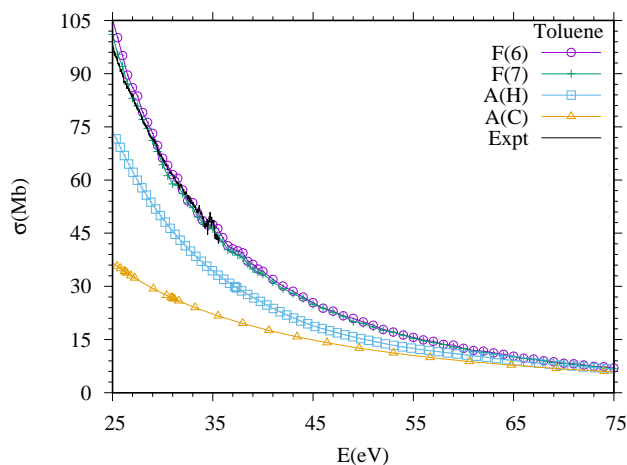


FIG. 4. Photoabsorption cross-sections of toluene. The experimental data is from Ref. 27.

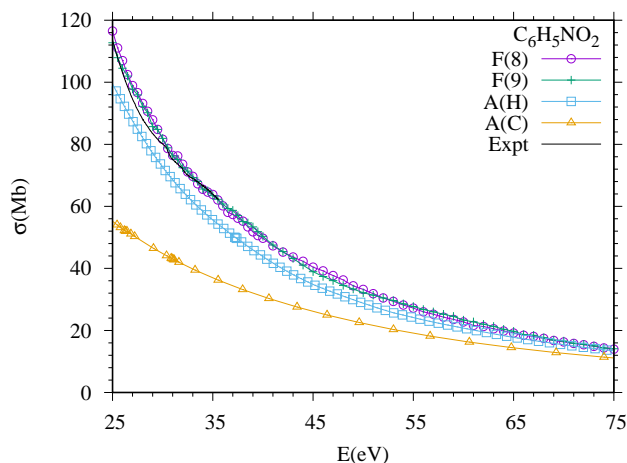


FIG. 5. Photoabsorption cross-sections of nitrobenzene. The experimental data is from Ref. 36.

2. Where direct measurements are available, the fragment-additive models $F(m)$ are noticeably more accurate than both the atom-additive models $A(H)$ and $A(C)$ except for hexafluorobenzene where $A(H)$ is comparable to $F(4)$ down to about 30 eV.
3. As noted by Au *et al.*,⁶⁰ chemical intuition is not always helpful in predicting which fragment model is more accurate. For example, $F(3)$ is more accurate than $F(2)$ even though one might expect $F(3)$ to be less accurate because the triple bonds in the nitrogen and ethyne molecules are unrepresentative of the bonding in the aromatic ring.
4. The $A(H)$ model is consistently better than $A(C)$ especially at lower energies, perhaps because the free-atom data used in $A(C)$ are based on the Hartree-Fock approximation which neglects electronic correlation.
5. The $A(H)$ model begins to converge to the fragment models at energies larger than about 65 eV. It can be used with confidence for $E > 200$ eV where the Brion data³⁸ and hence our fragment models end.

B. DOSDs

DOSDs for the eight (hetero)aromatic molecules were obtained with the methods and data described in Sec. II. The number of distributions examined ranged from 14 for pyridazine for which all the available experimental data comes from a single source¹⁸ to 112 for benzene for which there is ample data. The standard deviation s of the scale factors measures the consistency of the initial data and gives a rough idea of the accuracy of the DOSD. By this indicator, the benzene DOSD is the most accurate; the value of $100s = 0.5$ obtained for benzene in this work is less than a quarter of the value $100s = 2.2$ found⁶¹ for the benzene DOSD constructed decades earlier.⁹ Interestingly, unlike the older one, the best benzene DOSD of this work does not include any refractivity constraints. The DOSD for pyrazine is the least accurate ($100s=3.1$) and the values of $100s$ for the other six molecules are 1.2, 1.3, 1.5, 1.8, 1.8, and 2.2 for toluene, nitrobenzene, *s*-triazine, pyridazine, hexafluorobenzene, and pyrimidine, respectively. The integrated properties of the DOSDs are expected to be more accurate than the point-wise distributions.^{3,52}

C. Polarizabilities and refractivities

The DOSD polarizabilities $\alpha(\omega)$ for smaller frequencies are expected to have errors no larger than $\pm 1\%$ for benzene, $\pm 3\%$ for pyrazine, and $\pm 2\%$ for the remaining six molecules. Of the properties mentioned in Sec. II D, the one studied the most is the static polarizability $\alpha(0)$

TABLE I. Static electronic dipole polarizabilities α (in au). Multiply by 0.1481847 to get the polarizability volume in \AA^3 .

Molecule	B3LYP ^a	ω B97X-D ^b	<i>Ab initio</i>	DOSD ^f
Benzene	69.31	68.26	68.49 ^c	68.19 ^g
Pyridazine	58.93	58.00	58.73 ^c	57.09
Pyrimidine	58.23	57.32	57.81 ^c	57.00
Pyrazine	59.16	58.23	58.83 ^c	57.10
<i>s</i> -Triazine	52.42	51.67	52.76 ^d	52.17
Toluene	82.97	81.44	82.19 ^e	83.31
C ₆ H ₅ NO ₂	87.93	85.63	87.42 ^e	90.09
C ₆ F ₆	72.79	71.45	—	71.40

^a Global hybrid density functional: B3LYP/aug-cc-pVTZ, Ref. 64.

^b Range-separated hybrid density functional: ω B97X-D/aug-cc-pVTZ, Ref. 65.

^c Coupled-cluster method: CC3/aug-cc-pVTZ, Ref. 63.

^d Composite (hybrid) SDQ-MP4 value, Ref. 66.

^e 2nd order Møller-Plesset perturbation theory: MP2/aug-cc-pVTZ, Ref. 65.

^f This work.

^g The old DOSD result of Kumar and Meath⁹ is 67.79 au.

usually denoted simply as α . Consider benzene first. The current DOSD value of $S(-2) = \alpha = 68.19$ au is 0.6% larger than and supersedes both the older DOSD value⁹ and identical recommended value⁶² of 67.79 au. Table I compares the values of α obtained in this work with prior theoretical computations. The density functional theory (DFT) result from the global hybrid functional B3LYP is 1.6% larger than the DOSD value whereas the α computed with the range-separated hybrid functional ω B97X-D is within 0.1% of the DOSD value. The *ab initio* value obtained⁶³ with the CC3 coupled-cluster method is just 0.4% too large for benzene.

Now consider trends for the eight molecules. As expected,^{67–69} the B3LYP polarizabilities are consistently larger than all the other values. Somewhat unexpectedly, the ω B97X-D are consistently closer to the DOSD values than the CC3 values are for benzene and the diazines. The largest discrepancies, 3% for CC3 and 2% for ω B97X-D, occur for pyrazine whose DOSD is more poorly determined than the DOSDs for the other molecules. Comparison of the DOSD polarizabilities with their free-atom additive model counterparts, based on the exact⁷⁰ polarizability for H and accurate coupled-cluster values for the C, N, O, and F atoms,⁷¹ shows that all eight molecules satisfy the minimum polarizability principle^{72,73} as more than 97% of all molecules do.⁷⁴

Next, turn to the frequency-dependent polarizability $\alpha(\omega)$ and to the related molar refractivity $R(\omega)$ given by

$$R(\omega) = \frac{4\pi a_0^3}{3} N_A \alpha(\omega) \quad (15)$$

in which N_A is Avogadro's constant and a_0 is the Bohr radius. Table II shows that the molar refractivities predicted by the benzene DOSD are about 0.1% larger than

TABLE II. Molar refractivity R (in $\text{cm}^3\text{mol}^{-1}$) as a function of wave length λ (in nm) for benzene.

λ (nm)	DOSD ^a	Experiment ^b
644.02	26.32	26.19
546.23	26.68	26.54
508.72	26.88	26.75
480.13	27.07	26.96
435.96	27.45	27.36

^a This work.

^b Ref. 40.

TABLE III. Frequency-dependent polarizability $\alpha(\omega)$ (in au) as a function of wave length λ (in nm).

Molecule	Method	$\lambda = 632$ nm	$\lambda = 488$ nm
Benzene	CC3 ^a	70.86	72.63
	DOSD ^b	70.51	72.26
Pyridazine	CC3 ^a	60.62	62.07
	DOSD ^b	58.76	60.01
Pyrimidine	CC3 ^a	59.76	61.11
	DOSD ^b	58.74	60.04
Pyrazine	CC3 ^a	60.89	62.50
	DOSD ^b	59.09	60.64
<i>s</i> -Triazine	DOSD ^b	53.65	54.77
Toluene	DOSD ^b	86.16	88.31
C ₆ H ₅ NO ₂	DOSD ^b	93.65	96.46
C ₆ F ₆	DOSD ^b	73.32	74.77

^a Coupled-cluster method: CC3/aug-cc-pVTZ, Ref. 63.

^b This work.

the measured values⁴⁰ at all five wave lengths. This close agreement comes about even though the best DOSD does not have a refractivity constraint. The small discrepancies of 0.1% imply that there is a small incompatibility between the refractivity data⁴⁰ and the low energy photoabsorption cross-sections^{10–12,14} for benzene. There are no measured gas-phase refractivities for the other seven molecules.

Table III lists $\alpha(\omega)$ predicted by the DOSDs at two wave lengths and compares them with CC3 values where available.⁶³ Observe that the CC3 values are consistently larger than the DOSD values at both wave lengths. The CC3 and DOSD values differ by only 0.5%, 3%, 2%, and 3% for benzene, pyridazine, pyrimidine, and pyrazine respectively. These discrepancies are within the uncertainty of the DOSD polarizabilities except for pyridazine.

D. Sum rules and mean excitation energies

The dipole sum rules $S(k)$ for $-6 \leq k \leq 2$ are listed in Table IV. Many important physical proper-

TABLE IV. Dipole sum rules $S(k)$ (in au). $A(n)$ denotes $A \times 10^n$.

Molecule	$S(2)$	$S(1)$	$S(0)$	$S(-1)$	$S(-2)$	$S(-3)$	$S(-4)$	$S(-5)$	$S(-6)$
Benzene	1.947(4)	297.4	42	39.93	68.19	152.8	420.6	1338	4659
Pyridazine	2.515(4)	338.9	42	36.03	57.09	118.9	304.8	912.6	3043
Pyrimidine	2.517(4)	339.6	42	35.86	57.00	120.4	315.4	968.0	3311
Pyrazine	2.524(4)	342.5	42	35.48	57.10	125.9	355.7	1211	4714
<i>s</i> -Triazine	2.799(4)	359.7	42	34.11	52.17	106.2	269.4	811.8	2801
Toluene	2.280(4)	350.8	50	48.37	83.31	186.9	515.0	1650	5828
C ₆ H ₅ NO ₂	4.624(4)	553.9	64	54.18	90.09	209.3	629.1	2278	9339
C ₆ F ₆	1.215(5)	1023	90	55.46	71.40	136.3	348.9	1083	3740

ties are related³ to the $S(k)$. The Taylor expansion of the frequency-dependent polarizability $\alpha(\omega)$ valid for frequencies ω below the lowest excitation frequency ω_1 is

$$\alpha(\omega) = S(-2) + \omega^2 S(-4) + \omega^4 S(-6) + \dots \quad (16)$$

in which $S(-2) = \alpha(0)$ is the static electronic dipole polarizability and the $S(-2k-2)$ with $k = 1, 2, \dots$ are called Cauchy moments. $S(2)$ is proportional to the sum of the electron density values at the nuclei, and $S(-1)$ is related to the total differential cross-section for inelastic scattering in collisions of charged-particles with the molecule.

As can be verified in Table IV, the DOSDs are constrained to satisfy the KRT sum rule: $S(0) = N_e$ where N_e is the number of electrons in the molecule. The benzene $S(k)$ reported by Kumar and Meath⁹ differ from those in Table IV by 4.6% and 4.3% for $k = 2$ and 1, respectively, and by -1.8%, -0.6%, 0.8%, 2.3%, 4.0%, and 5.9% for $k = -1$ to $k = -6$, respectively.

The mean excitation energies $I(k)$ are listed in Table V. The average energy associated with the total inelastic scattering cross-section for grazing collisions of fast charged particles with the target species is $I(-1)$. The average energies $I(0)$ and $I(1)$ which are respectively related to the average energy loss (stopping power) and its mean fluctuation (straggling) in these collisions are required in radiation damage theory. $I(2)$ is related to the Lamb shift. The benzene $I(k)$ reported by Kumar and Meath⁹ differ from those in Table V by 4.7%, -0.4%, 5.9%, -0.8% and -1.2% for $k = 2, 1, 0, -1$, and -2 respectively.

E. Dispersion coefficients

The ten-term pseudospectra given in the supplementary material were used to calculate the spherically averaged C_6 dispersion coefficients listed in Table VI for interactions between pairs of the eight (hetero)aromatic molecules. The uncertainties in the C_6 coefficients are estimated to be in the $\pm 4\%$ to $\pm 8\%$ range depending upon the quality of the underlying DOSDs for the two species involved. The current value of 1765 au for ben-

TABLE V. Mean excitation energies $I(k)$ (in eV). $A(n)$ denotes $A \times 10^n$.

Molecule	$I(2)$	$I(1)$	$I(0)$	$I(-1)$	$I(-2)$
Benzene	9.976(3)	597.4	56.93	19.06	13.72
Pyridazine	1.148(4)	674.2	64.79	20.68	14.76
Pyrimidine	1.146(4)	673.5	65.17	20.72	14.63
Pyrazine	1.140(4)	672.0	66.32	20.73	14.24
<i>s</i> -Triazine	1.205(4)	708.9	69.17	21.60	15.18
Toluene	9.908(3)	594.4	55.95	18.80	13.67
C ₆ H ₅ NO ₂	1.299(4)	744.3	67.62	20.33	13.63
C ₆ F ₆	1.952(4)	993.2	92.19	27.24	17.03

zene is 2.4% larger than and supersedes the older value⁹ of $C_6 = 1723$ au.

Induced-dipole-induced-dipole C_6 coefficients are essential ingredients in the construction of model, non-retarded, intermolecular potentials that are valid for all intermolecular distances.⁷⁵ Moreover, they can assist in the calibration of calculated intermolecular potentials.⁷⁶ If the first two dispersion coefficients C_6 and C_8 in the long-range interaction energy expansion $V(R) = -C_6/R^6 - C_8/R^8 - C_{10}/R^{10} - \dots$ are available, then C_{10} and higher-order coefficients can be calculated to good accuracy from simple models.^{77,78}

The supplementary material lists $C_6(\text{A-B})$ coefficients for unlike ($\text{A} \neq \text{B}$) interactions in which A is one of the eight aromatic molecules considered here and B is one of 75 other species for which published pseudospectra are available.⁷⁹ These 600 C_6 coefficients together with those in Table VI constitute a moderately large, self-consistent set of C_6 coefficients. This test set facilitates a timely, contemporary assessment of a well-regarded^{7,80-83} approximation:

$$C_6(\text{A-B}) = \frac{2C_6(\text{A-A})C_6(\text{B-B})\alpha_{\text{A}}\alpha_{\text{B}}}{C_6(\text{A-A})\alpha_{\text{B}}^2 + C_6(\text{B-B})\alpha_{\text{A}}^2}, \quad (17)$$

in which α_{A} and α_{B} are the mean static polarizabilities of species A and B, respectively. Equation (17) is sometimes called the Moelwyn-Hughes combination rule because it was published first in his textbook.⁸⁴ However, it is quite

TABLE VI. Dispersion coefficients $C_6(A-B)$ (in au). Multiplication of an entry by 6934 yields a value in $K \text{ \AA}^6$.

A-B	C_6	A-B	C_6
Benzene-Benzene	1765	Pyrimidine-Toluene	1857
Benzene-Pyridazine	1531	Pyrimidine- $C_6H_5NO_2$	2009
Benzene-Pyrimidine	1523	Pyrimidine- C_6F_6	1775
Benzene-Pyrazine	1507	Pyrazine-Pyrazine	1288
Benzene-s-Triazine	1419	Pyrazine-s-Triazine	1213
Benzene-Toluene	2153	Pyrazine-Toluene	1838
Benzene- $C_6H_5NO_2$	2328	Pyrazine- $C_6H_5NO_2$	1988
Benzene- C_6F_6	2050	Pyrazine- C_6F_6	1756
Pyridazine-Pyridazine	1330	s-Triazine-s-Triazine	1143
Pyridazine-Pyrimidine	1323	s-Triazine-Toluene	1730
Pyridazine-Pyrazine	1308	s-Triazine- $C_6H_5NO_2$	1872
Pyridazine-s-Triazine	1233	s-Triazine- C_6F_6	1657
Pyridazine-Toluene	1867	Toluene-Toluene	2625
Pyridazine- $C_6H_5NO_2$	2020	Toluene- $C_6H_5NO_2$	2838
Pyridazine- C_6F_6	1785	Toluene- C_6F_6	2498
Pyrimidine-Pyrimidine	1315	$C_6H_5NO_2$ - $C_6H_5NO_2$	3070
Pyrimidine-Pyrazine	1301	$C_6H_5NO_2$ - C_6F_6	2707
Pyrimidine-s-Triazine	1226	C_6F_6 - C_6F_6	2416

likely that Eq. (17) was known prior to that because it follows rather simply from the London approximation^{85,86} for C_6 . All that is needed is to eliminate the Unsöld average energies from Eq. (13') in London's later paper⁸⁷ using his Eq. (13) from the same paper.⁸⁷

The mean absolute percent deviation of Eq. (17) from the DOSD values is only 0.23%. The predictions of Eq. (17) are in error by less than 1% in 606 (96.4%) of the 628 cases, and the error does not exceed 2.25% in the worst case. Interestingly, Eq. (17) is more likely to underestimate than overestimate the DOSD value; it predicts an underestimate in 400 of the 628 cases examined.

IV. WHAT NEXT?

The DOSDs constructed in this work for seven aromatic molecules plus the improved DOSD for benzene increase significantly the number of molecules for which reliable and complete DOSDs have been determined primarily from experimental photoabsorption data. None of the new DOSDs incorporate a refractivity constraint unlike many, if not most, DOSDs built in the past using various versions of the method used here. This is encouraging because there are not too many more molecules for which gas-phase refractivity data is available.⁶²

However, an examination of the MPI-Mainz UV/VIS Spectral Atlas³⁷ suggests that photoabsorption data from the absorption threshold to at least 30 eV, a range sufficient to construct a complete DOSD, is available for only about 20 more molecules. Once DOSDs for them are con-

structed, as they surely will be in the near future, what is the avenue for further progress? Obviously, experimental measurement of photoabsorption cross-sections for more species is one.

A different path is to find robust, black-box-like, additive models that are sufficiently accurate in the 10 eV to 30 eV range. That would open up the possibility of constructing complete DOSDs for the hundreds of molecules for which photoabsorption cross-sections are available³⁷ in a restricted energy range from the absorption threshold up to about 10 eV. Free-atom and fragment additive models are at levels 1 and 4 in the additive model hierarchy.⁴¹ Level 2 additive models using dressed atoms and level 3 models based on atoms that depend upon their environment deserve a closer look for photoabsorption cross-sections. Preliminary work along these lines is under way.

SUPPLEMENTARY MATERIAL

See the supplementary material for tables of $C_6(A-B)$ coefficients for unlike ($A \neq B$) interactions in which A is one of the eight aromatic molecules treated in this work and B is one of 75 other species, ten-term pseudospectra for the eight aromatic molecules, and references to the published pseudospectra for the 75 other species.

DATA AVAILABILITY

The data that supports the findings of this study are available within the article and its supplementary material.

- ¹M. Stöhr, T. V. Voorhis, and A. Tkatchenko, "Theory and practice of modeling van der Waals interactions in electronic-structure calculations," *Chem. Soc. Rev.* **48**, 4118–4154 (2019).
- ²H. Margenau, "Note on the calculation of van der Waals forces," *Phys. Rev.* **37**, 1425–1430 (1931).
- ³A. J. Thakkar, "Construction of constrained dipole oscillator strength distributions," *Z. Phys. Chemie* **230**, 633–650 (2016).
- ⁴A. Dalgarno, "New methods for calculating long-range intermolecular forces," *Adv. Chem. Phys.* **12**, 143–166 (1967).
- ⁵G. D. Zeiss, W. J. Meath, J. C. F. MacDonald, and D. J. Dawson, "Dipole oscillator strength distributions, sums, and some related properties for Li, N, O, H₂, N₂, O₂, NH₃, H₂O, NO, and N₂O," *Can. J. Phys.* **55**, 2080–2100 (1977).
- ⁶A. Kumar, W. J. Meath, P. Bündgen, and A. J. Thakkar, "Reliable anisotropic dipole properties, and dispersion energy coefficients, for O₂ evaluated using constrained dipole oscillator strength techniques," *J. Chem. Phys.* **105**, 4927–4937 (1996).
- ⁷T. N. Olney, N. M. Cann, G. Cooper, and C. E. Brion, "Absolute scale determination for photoabsorption spectra and the calculation of molecular properties using dipole sum-rules," *Chem. Phys.* **223**, 59–98 (1997).
- ⁸J. Berkowitz, *Atomic and Molecular Photoabsorption: Absolute Total Cross Sections* (Academic, San Diego, 2002).
- ⁹A. Kumar and W. J. Meath, "Dipole oscillator strength properties and dispersion energies for acetylene and benzene," *Mol. Phys.* **75**, 311–324 (1992).

- ¹⁰E. E. Rennie, C. A. F. Johnson, J. E. Parker, D. M. P. Holland, D. A. Shaw, and M. A. Hayes, "A photoabsorption, photodissociation and photoelectron spectroscopy study of C₆H₆ and C₆D₆," *Chem. Phys.* **229**, 107–123 (1998).
- ¹¹T. Etzkorn, B. Klotz, S. Sørensen, I. V. Patroescu, I. Barnes, K. H. Becker, and U. Platt, "Gas-phase absorption cross sections of 24 monocyclic aromatic hydrocarbons in the UV and IR spectral ranges," *Atmos. Environ.* **33**, 525–540 (1999).
- ¹²R. Feng, G. Cooper, and C. E. Brion, "Dipole (e,e) spectroscopic studies of benzene: quantitative photoabsorption in the UV, VUV and soft X-ray regions," *J. Elect. Spectrosc. Relat. Phenom.* **123**, 199–209 (2002).
- ¹³S. Fally, M. Carleer, and A. C. Vandaele, "UV Fourier transform absorption cross sections of benzene, toluene, meta-, ortho-, and para-xylene," *J. Quant. Spectrosc. Radiat. Transfer* **110**, 766–782 (2009).
- ¹⁴F. Capalbo, Y. Bénilan, N. Fray, M. Schwell, N. Champion, E. Es-sebbar, T. Koskinen, I. Lehecka, and R. Yelle, "New benzene absorption cross sections in the VUV, relevance for Titan's upper atmosphere," *Icarus* **265**, 95–109 (2016).
- ¹⁵A. Dawes, N. Pascual, S. V. Hoffmann, N. C. Jones, and N. J. Mason, "Vacuum ultraviolet photoabsorption spectroscopy of crystalline and amorphous benzene," *Phys. Chem. Chem. Phys.* **19**, 27544–27555 (2017).
- ¹⁶B. L. Jhanwar, W. J. Meath, and J. C. F. MacDonald, "Dipole oscillator strength distributions and sums for C₂H₆, C₃H₈, *n*-C₄H₁₀, *n*-C₅H₁₂, *n*-C₆H₁₄, *n*-C₇H₁₆, and *n*-C₈H₁₈," *Can. J. Phys.* **59**, 185–197 (1981).
- ¹⁷A. Kumar and A. J. Thakkar, "Constrained dipole oscillator strength distributions for CF₄, CClF₃, CCl₂F₂, CCl₃F, CHF₃, CH₃F, CH₃Cl, CH₃Br, CH₃I, C₂F₆, and CCl₃CF₃," *Z. Phys. Chemie* **230**, 1473–1486 (2016).
- ¹⁸D. M. P. Holland, D. A. Shaw, S. Coriani, M. Stener, and P. Decleva, "A study of the valence shell electronic states of pyridazine by photoabsorption spectroscopy and time-dependent density functional theory calculations," *J. Phys. B: At. Mol. Opt. Phys.* **46**, 175103 (2013).
- ¹⁹A. Bolvinos, P. Tsekeris, J. Philis, E. Pantos, and G. Andritsopoulos, "Absolute vacuum ultraviolet absorption spectra of some gaseous azabenzenes," *J. Mol. Spectrosc.* **103**, 240–256 (1984).
- ²⁰F. F. da Silva, D. Almeida, G. Martins, A. R. Milosavljevic, B. P. Marinkovic, S. V. Hoffmann, N. J. Mason, Y. Nunes, G. Garcia, and P. Limão-Vieira, "The electronic states of pyrimidine studied by VUV photoabsorption and electron energy-loss spectroscopy," *Phys. Chem. Chem. Phys.* **12**, 6717–6731 (2010).
- ²¹M. Stener, P. Decleva, D. M. P. Holland, and D. A. Shaw, "A study of the valence shell electronic states of pyrimidine and pyrazine by photoabsorption spectroscopy and time-dependent density functional theory calculations," *J. Phys. B: At. Mol. Opt. Phys.* **44**, 075203 (2011).
- ²²D. M. P. Holland, D. A. Shaw, M. Stener, P. Decleva, and S. Coriani, "A study of the valence shell electronic states of s-triazine by photoabsorption spectroscopy and ab initio calculations," *Chem. Phys.* **477**, 96–104 (2016).
- ²³A. Bolvinos, J. Philis, E. Pantos, P. Tsekeris, and G. Andritsopoulos, "The methylbenzenes vis-a-vis benzene. Comparison of their spectra in the Rydberg series region," *J. Chem. Phys.* **75**, 4343–4349 (1981).
- ²⁴A. Bolvinos, J. Philis, E. Pantos, P. Tsekeris, and G. Andritsopoulos, "The methylbenzenes vis-à-vis benzene. Comparison of their spectra in the valence shell transition region," *J. Mol. Spectrosc.* **94**, 55–68 (1982).
- ²⁵H. Hippler, J. Troe, and H. J. Wendelken, "UV absorption spectra of vibrationally highly excited toluene molecules," *J. Chem. Phys.* **78**, 5351–5357 (1983).
- ²⁶S. A. A. E.-A. Shama, *Vacuum ultraviolet absorption spectra of organic compounds in gaseous and liquid state*, Ph.D. thesis, Zagazig University, Egypt (1991).
- ²⁷D. A. Shaw, D. M. P. Holland, M. A. MacDonald, M. A. Hayes, L. G. Shpinkova, E. E. Rennie, C. A. F. Johnson, J. E. Parker, and W. von Niessen, "An experimental and theoretical study of the spectroscopic and thermodynamic properties of toluene," *Chem. Phys.* **230**, 97–116 (1998).
- ²⁸W. Koban, J. D. Koch, R. K. Hanson, and C. Schulz, "Absorption and fluorescence of toluene vapor at elevated temperatures," *Phys. Chem. Chem. Phys.* **6**, 2940–2945 (2004).
- ²⁹G. El Dib, A. Chakir, E. Roth, J. Brion, and D. Daumont, "Study of benzylperoxy radical using laser photolysis: Ultraviolet spectrum, self-reaction, and reaction with HO₂ kinetics," *J. Phys. Chem. A* **110**, 7848–7857 (2006).
- ³⁰C. Serralheiro, D. Duflot, F. F. da Silva, S. V. Hoffmann, N. C. Jones, N. J. Mason, B. Mendes, and P. Limão-Vieira, "Toluene valence and Rydberg excitations as studied by *ab initio* calculations and vacuum ultraviolet (VUV) synchrotron radiation," *J. Phys. Chem. A* **119**, 9059–9069 (2015).
- ³¹J. Philis, A. Bolvinos, G. Andritsopoulos, E. Pantos, and P. Tsekeris, "A comparison of the absorption spectra of the fluorobenzenes and benzene in the region 4.5–9.5 eV," *J. Phys. B: At. Mol. Phys.* **14**, 3621–3635 (1981).
- ³²C. Motch, A. Giuliani, J. Delwiche, P. Limão-Vieira, N. J. Mason, S. V. Hoffmann, and M.-J. Hubin-Franskin, "Electronic structure of hexafluorobenzene by high-resolution vacuum ultraviolet photo-absorption and He(I) photoelectron spectroscopy," *Chem. Phys.* **328**, 183–189 (2006).
- ³³D. M. P. Holland, D. A. Shaw, M. Stener, and P. Decleva, "A study of the valence shell electronic structure of hexafluorobenzene using photoabsorption and photoelectron spectroscopy, and TDDFT calculations," *J. Phys. B: At. Mol. Opt. Phys.* **42**, 245201 (2009).
- ³⁴S. Nagakura, M. Kojima, and Y. Maruyama, "Electronic spectra and electronic structures of nitrobenzene and nitromesitylene," *J. Mol. Spectrosc.* **13**, 174–192 (1964).
- ³⁵L. Frøsig, O. J. Nielsen, M. Bilde, T. J. Wallington, J. J. Orlando, and G. S. Tyndall, "Kinetics and mechanism of the reaction of Cl atoms with nitrobenzene," *J. Phys. Chem. A* **104**, 11328–11331 (2000).
- ³⁶L. Cooper, L. G. Shpinkova, E. E. Rennie, D. M. P. Holland, and D. A. Shaw, "Time-of-flight mass spectrometry study of the fragmentation of valence shell ionised nitrobenzene," *Int. J. Mass Spectrom.* **207**, 223–239 (2001).
- ³⁷H. Keller-Rudek, G. K. Moortgat, R. Sander, and R. Sørensen, "The MPI-Mainz UV/VIS spectral atlas of gaseous molecules of atmospheric interest," *Earth System Science Data* **5**, 365–373 (2013).
- ³⁸C. E. Brion, "Database of Absolute Dipole Photoabsorption Oscillator Strengths of Atoms and Small Molecules," <https://www.chem.ubc.ca/chris-brion>, last accessed 2020-06-28.
- ³⁹P. Hölemann and H. Goldschmidt, "Über die Refraktion und Dispersion einiger dampfförmiger Halogenide von Elementen der vierten Gruppe des periodischen Systems in sichtbaren Gebiet. 6. Mitteilung über Refraktion und Dispersion von Gasen und Dämpfen," *Z. physik. Chemie B* **24**, 199–209 (1934).
- ⁴⁰K. L. Ramaswamy, "Refractive indices and dispersions of gases and vapours. Substituted methanes and ethane, cyclopropane, ethylene oxide and benzene," *Proc. Ind. Acad. Sci. A* **4**, 675–686 (1936).
- ⁴¹In the context of photoabsorption cross-sections, additive models are sometimes called mixture rules. A succinct history and description of additive models is given in A. J. Thakkar, "A hierarchy for additive models of polarizability," *AIP Conf. Proc.* **1504**, 586–589 (2012). This paper set up a hierarchy of additive models to help clarify what can be expected from a model in a given level of the hierarchy.
- ⁴²B. L. Henke, E. M. Gullikson, and J. C. Davis, "X-ray interactions: photoabsorption, scattering, transmission, and reflection at $E = 50$ –30,000 eV, $Z = 1$ –92," *At. Data Nucl. Data Tables* **54**, 181–342 (1993). The data is available digitally from

- https://henke.lbl.gov/optical_constants/asf.html which also reports a few updates to the published work.
- ⁴³C. T. Chantler, "Theoretical form factor, attenuation and scattering tabulation for $Z = 1-92$ from $E = 1-10$ eV to $E = 0.4-1.0$ MeV," *J. Phys. Chem. Ref. Data* **24**, 71-643 (1995).
 - ⁴⁴R. J. Doerksen and A. J. Thakkar, "Polarizabilities of heteroaromatic molecules: Azines revisited," *Int. J. Quantum Chem.* **60**, 1633-1642 (1996).
 - ⁴⁵S. Tixier, G. Cooper, R. Feng, and C. E. Brion, "Measurement of absolute dipole oscillator strengths for pyridine: photoabsorption and the molecular and dissociative photoionization in the valence shell (4-200 eV)," *J. Elect. Spect. Relat. Phenom.* **123**, 185-197 (2002).
 - ⁴⁶W. F. Chan, G. Cooper, R. N. S. Sodhi, and C. E. Brion, "Absolute optical oscillator-strengths for discrete and continuum photoabsorption of molecular nitrogen (11-200 eV)," *Chem. Phys.* **170**, 81-97 (1993).
 - ⁴⁷G. Cooper, G. R. Burton, and C. E. Brion, "Absolute UV and soft X-ray photoabsorption of acetylene by high resolution dipole (e,e) spectroscopy," *J. Elect. Spect. Relat. Phenom.* **73**, 139-148 (1995).
 - ⁴⁸T. N. Olney, G. Cooper, W. F. Chan, G. R. Burton, C. E. Brion, and K. H. Tan, "Quantitative studies of the photoabsorption, photoionization, and ionic photofragmentation of methyl fluoride at VUV and soft X-ray energies (7-250 eV) using dipole electron scattering and synchrotron radiation," *Chem. Phys.* **189**, 733-756 (1994).
 - ⁴⁹J. W. Au and C. E. Brion, "Absolute oscillator strengths for the valence-shell photoabsorption (2-200 eV) and the molecular and dissociative photoionization (11-80 eV) of nitrogen dioxide," *Chem. Phys.* **218**, 109-126 (1997).
 - ⁵⁰J. W. Au, G. R. Burton, and C. E. Brion, "Quantitative spectroscopic studies of the valence-shell electronic excitation of Freons (CFCl_3 , CF_2Cl_2 , CF_3Cl , and CF_4) in the VUV and soft X-ray regions," *Chem. Phys.* **221**, 151-168 (1997).
 - ⁵¹J. W. Au, G. Cooper, G. R. Burton, T. N. Olney, and C. E. Brion, "The valence shell photoabsorption of the linear alkanes, $\text{C}_n\text{H}_{2n+2}$ ($n = 1-8$): absolute oscillator strengths (7-220 eV)," *Chem. Phys.* **173**, 209-239 (1993). Erratum, *ibid.*, **178**, 615 (1993).
 - ⁵²A. Kumar and W. J. Meath, "Dipole oscillator strength distributions, properties and dispersion energies for the dimethyl, diethyl and methyl-propyl ethers," *Mol. Phys.* **106**, 1531-1544 (2008).
 - ⁵³A. Kumar and A. J. Thakkar, "Dipole oscillator strength distributions with improved high-energy behavior: Dipole sum rules and dispersion coefficients for Ne, Ar, Kr, and Xe revisited," *J. Chem. Phys.* **132**, 074301 (2010).
 - ⁵⁴A. Kumar and A. J. Thakkar, "Dipole polarizability, sum rules, mean excitation energies, and long-range dispersion coefficients for buckminsterfullerene C_{60} ," *Chem. Phys. Lett.* **516**, 208-211 (2011).
 - ⁵⁵A. Kumar and A. J. Thakkar, "Dipole properties of PH_3 , PF_3 , PF_5 , PCl_3 , SiCl_4 , GeCl_4 , and SnCl_4 ," *Mol. Phys.* **114**, 1657-1663 (2016).
 - ⁵⁶A. Kumar and A. J. Thakkar, "Constrained dipole oscillator strength distributions, sum rules, and dispersion coefficients for Br_2 and BrCN ," *Chem. Phys. Lett.* **672**, 31-33 (2017).
 - ⁵⁷T. Koga and A. J. Thakkar, "Moments and expansion coefficients of atomic electron momentum densities: numerical Hartree-Fock calculations for hydrogen to lawrencium," *J. Phys. B: At. Mol. Opt. Phys.* **29**, 2973-2983 (1996). $\rho(0)$ is calculated from the atomic number Z and values of b_8 listed in Table 2 of their work using the relation: $\rho(0) = \pi b_8 Z^3/8$.
 - ⁵⁸J. A. Shohat and J. D. Tamarkin, *The problem of moments* (American Mathematical Society, New York, 1943).
 - ⁵⁹H. B. G. Casimir and D. Polder, "The influence of retardation on the London-van der Waals forces," *Phys. Rev.* **73**, 360-372 (1948).
 - ⁶⁰J. W. Au, G. Cooper, G. R. Burton, and C. E. Brion, "An evaluation of atomic and molecular mixture rules and group additivity concepts for the estimation of radiation absorption by long-chained, saturated hydrocarbons at vacuum UV and soft X-ray energies," *Chem. Phys.* **187**, 305-316 (1994).
 - ⁶¹100s is the same as the quantity STD used in DOSD work by Meath and coworkers.
 - ⁶²U. Hohm, "Experimental static dipole-dipole polarizabilities of molecules," *J. Mol. Struct.* **1054-1055**, 282-292 (2013).
 - ⁶³M. W. Jørgensen, R. Faber, A. Ligabue, and S. P. A. Sauer, "Benchmarking correlated methods for frequency-dependent polarizabilities: Aromatic molecules with the CC3, CCSD, CC2, SOPPA, SOPPA(CC2), and SOPPA(CCSD) methods," *J. Chem. Theory Comput.* **16**, 3006-3018 (2020).
 - ⁶⁴S. A. Blair and A. J. Thakkar, "Relating polarizability to volume, ionization energy, electronegativity, hardness, moments of momentum, and other molecular properties," *J. Chem. Phys.* **141**, 074306 (2014).
 - ⁶⁵R. D. Johnson, III, "NIST Computational Chemistry Comparison and Benchmark Database, Release 20," (August 2019), <https://cccbdb.nist.gov/introx.asp>, last accessed 2020-07-22.
 - ⁶⁶E. F. Archibong and A. J. Thakkar, "Polarizabilities of aromatic six-membered rings: azines and 'inorganic benzenes'," *Mol. Phys.* **81**, 557-567 (1994).
 - ⁶⁷A. L. Hickey and C. N. Rowley, "Benchmarking quantum chemical methods for the calculation of molecular dipole moments and polarizabilities," *J. Phys. Chem. A* **118**, 3678-3687 (2014).
 - ⁶⁸T. Wu, Y. N. Kalugina, and A. J. Thakkar, "Choosing a density functional for static molecular polarizabilities," *Chem. Phys. Lett.* **635**, 257-261 (2015).
 - ⁶⁹D. Hait and M. Head-Gordon, "How accurate are static polarizability predictions from density functional theory? An assessment over 132 species at equilibrium geometry," *Phys. Chem. Chem. Phys.* **20**, 19800-19810 (2018).
 - ⁷⁰P. S. Epstein, "The Stark effect from the point of view of Schrödinger's quantum theory," *Phys. Rev.* **28**, 695-710 (1926).
 - ⁷¹A. K. Das and A. J. Thakkar, "Static response properties of second-period atoms: coupled cluster calculations," *J. Phys. B: At. Mol. Opt. Phys.* **31**, 2215-2223 (1998).
 - ⁷²P. K. Chattaraj and S. Sengupta, "Popular electronic structure principles in a dynamical context," *J. Phys. Chem.* **100**, 16126-16130 (1996).
 - ⁷³Y. Simón-Manso and P. Fuentealba, "On the density functional relationship between static dipole polarizability and global softness," *J. Phys. Chem. A* **102**, 2029-2032 (1998).
 - ⁷⁴S. A. Blair and A. J. Thakkar, "How often is the minimum polarizability principle violated?" *Chem. Phys. Lett.* **556**, 346-349 (2013).
 - ⁷⁵R. J. Wheatley, A. S. Tulegenov, and E. Bichoutskaia, "Intermolecular potentials from supermolecule and monomer calculations," *Int. Rev. Phys. Chem.* **23**, 151-185 (2004).
 - ⁷⁶K. Szalewicz, "Symmetry-adapted perturbation theory of intermolecular forces," *WIREs Comput. Mol. Sci.* **2**, 254-272 (2012).
 - ⁷⁷A. J. Thakkar and V. H. Smith, Jr., "On a representation of the long-range interatomic interaction potential," *J. Phys. B: At. Mol. Phys.* **7**, L321-L325 (1974).
 - ⁷⁸A. J. Thakkar, "Higher dispersion coefficients: Accurate values for hydrogen atoms and simple estimates for other systems," *J. Chem. Phys.* **89**, 2092-2098 (1988).
 - ⁷⁹The 75 species are comprised of 7 monatomic, 10 diatomic, 9 triatomic, 11 inorganic, and 38 organic species. The original references to their published pseudospectra are enumerated in the supplementary material.
 - ⁸⁰K. T. Tang, "Dynamic polarizabilities and van der Waals coefficients," *Phys. Rev.* **177**, 108-114 (1969).
 - ⁸¹H. L. Kramer and D. R. Herschbach, "Combination rules for van der Waals force constants," *J. Chem. Phys.* **53**, 2792-2800 (1970).
 - ⁸²G. D. Zeiss and W. J. Meath, "Dispersion energy constants $\text{C}_6(\text{A,B})$, dipole oscillator strength sums and refractivities for Li, N, O, H_2 , N_2 , O_2 , NH_3 , H_2O , NO and N_2O ," *Mol. Phys.* **33**, 1155-1176 (1977).

- ⁸³A. J. Thakkar, "Bounding and estimation of van der Waals coefficients," J. Chem. Phys. **81**, 1919–1928 (1984).
- ⁸⁴E. A. Moelwyn-Hughes, *Physical chemistry* (Pergamon, New York, 1957) p. 332.
- ⁸⁵F. London, "Zur Theorie und Systematik der Molekularkräfte," Z. Physik **63**, 245–279 (1930).
- ⁸⁶An English translation of Ref. 85 can be found in H. Hettema, ed., *Quantum Chemistry: Classic Scientific Papers* (World Scientific, Singapore, 2000) pp. 369–399.
- ⁸⁷F. London, "The general theory of molecular forces," Trans. Faraday Soc. **33**, 8–26 (1937).